

Article

# Preparation of Durable Superhydrophobic Coatings Based on Discrete Adhesives

Xuejuan Liu <sup>1,2,3,\*</sup>, Zhiguo Zhou <sup>1,2</sup>, Ming Chen <sup>4</sup>, Zheng Liu <sup>1</sup>, Shuhui Jiang <sup>1</sup> and Lei Wang <sup>5,\*</sup>

<sup>1</sup> College of Life Science, Langfang Normal University, Langfang 065000, China

<sup>2</sup> Technical Innovation Center for Utilization of Edible and Medicinal Fungi, Langfang 065000, China

<sup>3</sup> Langfang Key Laboratory for Biological Sample Analysis and Pesticide Residue Detection, Langfang Normal University, Langfang 065000, China

<sup>4</sup> Institute of Advanced Structure Technology, Beijing Institute of Technology, Beijing 100081, China

<sup>5</sup> Beijing Key Laboratory of Lignocellulosic Chemistry, Beijing Forestry University, Beijing 100083, China

\* Correspondence: 1231941@lnf.edu.cn (X.L.); leiwangns@bjfu.edu.cn (L.W.)

**Abstract:** Due to the low adhesion observed at the interface between solid and liquid, superhydrophobic coatings hold significant promise for various applications, such as self-cleaning, anti-corrosion, anti-icing, and drag reduction. However, a notable challenge hindering their widespread adoption in these domains lies in their delicate durability. In this study, we propose a straightforward method for preparation. The fluorosilicone resin is initially discretized through a gradual introduction of nonsolvent into its solution, followed by thorough mixing and stirring with silica nanoparticles. The resulting mixture is then sprayed onto the substrate surface after drying, forming a self-similar, porous, and rough structure extending from top to bottom. This process yields a coating exhibiting excellent chemical and mechanical durability simultaneously. Using this approach, we achieved a superhydrophobic coating with a contact angle of 156° and a roll angle of 2.2°, with water droplet adhesion of only  $10.8 \pm 0.4 \mu\text{N}$ . Remarkably, the coating maintained excellent superhydrophobicity even after undergoing sandpaper abrasion (10 m), tape peeling (30 times), and prolonged water impact (60 min), showing its robust mechanical stability. Furthermore, following exposure to acid, alkali, and aqueous solutions (7 days), UV irradiation (10 days), and extreme temperature variations ( $-20^\circ\text{C}$  to  $80^\circ\text{C}$ ), the coatings retained their superhydrophobic properties and exhibited good chemical durability. This method offers a novel approach to enhance the durability and practicality of superhydrophobic coatings.



**Citation:** Liu, X.; Zhou, Z.; Chen, M.; Liu, Z.; Jiang, S.; Wang, L. Preparation of Durable Superhydrophobic Coatings Based on Discrete Adhesives. *Coatings* **2024**, *14*, 463. <https://doi.org/10.3390/coatings14040463>

Academic Editor: Carlo Antonini

Received: 24 March 2024

Revised: 7 April 2024

Accepted: 8 April 2024

Published: 11 April 2024



**Copyright:** © 2024 by the authors. Licensee MDPI, Basel, Switzerland. This article is an open access article distributed under the terms and conditions of the Creative Commons Attribution (CC BY) license (<https://creativecommons.org/licenses/by/4.0/>).

## 1. Introduction

Droplets on superhydrophobic surfaces exhibit an apparent contact angle exceeding 150° and a rolling angle below 10°, ensuring exceptionally low adhesion properties both vertically and horizontally [1–3]. This characteristic renders such surfaces highly advantageous for applications involving self-cleaning [4,5], anti-corrosion [6,7], anti-icing [8,9], and drag reduction [10,11].

Drawing insights from the study of natural superhydrophobic entities like lotus leaves and water striders, researchers have identified two pivotal factors: a rough surface structure and materials with low surface energy [12–15]. Inspired by this understanding, various methods have been proposed for fabricating superhydrophobic surfaces, including etching [16,17], templating [18,19], spraying [20], sol-gel processes [21–23], layer-by-layer self-assembly [24,25], electrochemical deposition [26,27], and others. Among these, the spraying technique has garnered significant attention due to its operational simplicity, minimal equipment and substrate requirements, and cost-effectiveness for large-scale production [28,29].

Although great progress has been made in the preparation of superhydrophobic coatings in the laboratory, they still face many challenges in practical applications. The primary limitation arises from the delicate microscopic rough structure of superhydrophobic coatings, which can be easily damaged by external forces or environmental factors, leading to a loss of their superhydrophobic properties. Consequently, there has been a growing focus on developing resilient superhydrophobic coatings [30,31].

Initially, many of the early spray methods for creating superhydrophobic coatings involved blending silicone or other resins with low surface energy modified nanoparticles directly in a solvent, then applying the mixture onto the desired substrate surface following agitation. Upon drying, the nanoparticles serve as a framework to establish a rough structure, which bonds to the substrate surface via the resin [32–35]. This approach is notably straightforward, facilitating mass production, and yields coatings with favorable superhydrophobic characteristics. However, its principal drawback lies in its limited mechanical durability, as even minor abrasion with sandpaper can compromise its superhydrophobic properties. The deficiency of this direct blending method is believed to stem from the embedding of nanoparticles within the resin, resulting in only the surface layer possessing a rough structure composed of nanoparticles [36–38]. Consequently, upon abrasion, this surface layer becomes exposed to the high surface energy resin, resulting in the loss of superhydrophobicity. To enhance coating durability, researchers have explored substituting rigid resins with flexible alternatives like PDMS [39] and ABS [40] post-drying, using the deformability of these materials to dissipate energy and minimize microstructural damage. While these investigations have succeeded in enhancing coating durability, prolonged abrasion gradually diminishes elasticity, leading to a deterioration in the mechanical resilience of such superhydrophobic coatings.

To enhance coating durability, Lu et al. [41] suggested initially applying a layer of adhesive onto the substrate surface, followed by spraying a nanoparticle solution onto the adhesive-coated surface to create a superhydrophobic coating upon drying. This method establishes a connection between the substrate and the rough structure formed by the nanoparticles through the intermediary adhesive layer. By circumventing nanoparticle embedding into the resin, this approach ensures that even if the surface's rough structure is compromised, the exposed new surface remains composed of low surface energy nanoparticles, thereby preserving better durability. However, due to the nature of this spraying technique, the bonding strength between the resin and the rough structure is low, making it susceptible to the detachment of the rough structure, consequently reducing the coating's lifespan.

Wang et al. [31] proposed the “arming” strategy, wherein micron-sized structures serve as protective armor for hydrophobic nanostructures, which can also be employed in spraying methodologies. In certain investigations, micron-sized structures like triangles and honeycombs were initially fabricated on the substrate surface, followed by the spraying of nanoparticles within these micron structures. Nevertheless, a notable drawback of this strategy is its reliance on costly and intricate techniques, such as photolithography for micron structure preparation. Subsequent research endeavors have combined these two strategies by initially applying a resin onto the substrate surface, followed by spraying micron particles to serve as armor, and subsequently applying nanoparticles to confer superhydrophobic properties [42]. While this combined approach has somewhat improved coating durability, it has not effectively addressed the issue of weak bonding between the rough structure and the resin.

This paper proposes a novel and straightforward method for fabricating superhydrophobic coatings to address the limitations of current preparation techniques. The process involves the dropwise addition of an unwanted solvent into a solution of fluorosilicone resin, which is then mixed with fluorine-modified silica nanoparticles and sprayed onto the substrate surface. Upon drying, the resulting coating exhibits low adhesion with a contact angle of  $156^\circ \pm 0.6^\circ$  and a roll angle of  $2.3^\circ \pm 0.3^\circ$ . To assess mechanical durability, we subjected the coating to abrasion testing using sandpaper (1000 mesh, 4.9 kPa) over

10 m, with the contact angle and rolling angle showing minimal change, indicating good abrasion resistance. Additionally, a water impact test (1.12 m/s flow rate, 20 cm from the sample) demonstrated excellent superhydrophobicity retention after 60 min. The coating also withstood tape peeling (3 M, 2.5 kPa) for 30 repetitions without failure. Chemical durability testing involved immersion in acid (pH = 1), neutral (pH = 7), and alkaline (pH = 12) salt solutions, as well as water solutions, UV irradiation (310 nm, 6 mW/cm<sup>2</sup>) for 10 days, and high and low-temperature stability tests (−20 °C to 80 °C) for 30 cycles, all of which resulted in the coatings remaining undamaged and maintaining superhydrophobicity, showing stable chemical durability. Consequently, our method offers a simple and effective approach, presenting a novel concept for producing durable superhydrophobic coatings.

## 2. Experiment

### 2.1. Materials and Reagents

The solvents used were 99.5% pure butyl acetate and 99.5% pure ethanol, both of which were purchased from Energy Chemical. The binder was fluorosilicone resin purchased from Fuxin Ruifeng Fluorochemical Co., Ltd. (Fuxin, China). The nanoparticles used were silica (20 nm particle size) purchased from Hubei Huifu Nanomaterials Co., Ltd. (Yichang, China). The nanoparticle modifiers used were 1H,1H,2H,2H-perfluorodecyltriethoxysilane (97% purity, PFDTES), ammonia, and tetraethoxysilane (TEOS), which were obtained from Shanghai Meryer Chemical Technology Co (Shanghai, China). The substrates used were tinplate sheets (12 × 7 cm<sup>2</sup>) with the chemical compositions Sn (51.49%), Fe (47.23%), Co (0.88%), and Al (0.41%). Before spraying, the sheets were rinsed with butyl acetate.

### 2.2. Silicon Dioxide Nanoparticle Modification Method

Initially, 20 g of nanoparticles were dissolved in 1 L of ethanol/ammonia solution (with a volume ratio of 23:2). After mixing and ultrasonication for 30 min, 3 mL of PFDTES and 3 mL of TEOS were added successively. Following a 2 h reaction at room temperature under vigorous stirring, a homogeneous sample was formed. Subsequently, the sample was washed with butyl acetate three times. Upon centrifugation and heat drying, fluorinated silica nanoparticles were obtained (Figure 1a).

### 2.3. Coating Preparation

Fluorosilicone resin (7 g) was dissolved in an appropriate amount of butyl acetate solution, ultrasonicated for 10 min, and stirred magnetically for 30 min. Under stirring conditions, the ethanol solvent was slowly added. The volume ratio of added butyl acetate to ethanol solvent was 1:3.5. Because the fluorosilicone resin was soluble in butyl acetate but insoluble in ethanol, phase separation occurred during the dropwise addition. Then, 2.6 g of fluorinated nanoparticles was added to the mixed solution and stirred magnetically for 2 h. The prepared mixed solution was poured into a spray gun, the pressure was adjusted to approximately 0.5 MPa, and the spray gun was placed perpendicular to the tinplate at 90° at a distance of approximately 20 cm and sprayed on the surface of the cleaned tinplate. The samples were placed in an oven at 120 °C for 2 h to obtain the superhydrophobic coating. A schematic diagram of the preparation process is shown in Figure 1b.

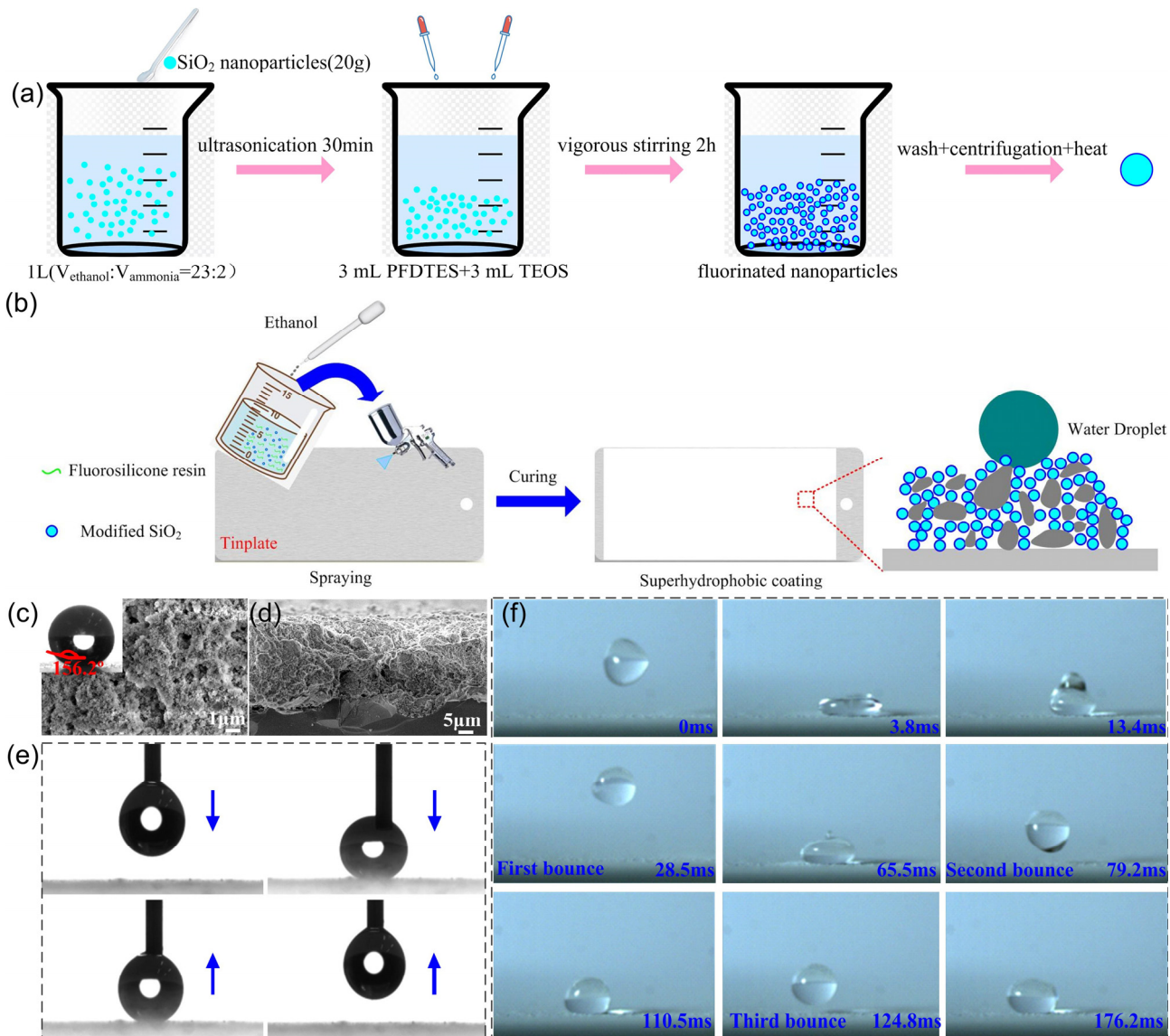


**Figure 1.** (a) Schematic diagram of the silicon dioxide nanoparticle modification method; (b) schematic diagram of the superhydrophobic coating preparation method; SEM images of the surface morphology of the prepared samples: (c) top view and (d) side view; (e) droplet adhesion test on the sample surface; (f) droplet bounce test on the sample surface.

#### 2.4. Characterization of Coating Properties

Apparent contact angle and roll angle measurements: These were measured using a contact angle meter (DSA 255, 5  $\mu\text{L}$  deionized water drop) (KRUSS, Hamburg, Germany), and their sizes were averaged from five different locations on the same sample. The abrasion resistance test utilized 1000 grit sandpaper, with a 200 g weight applied on the sandpaper as it moved at a constant speed across the sample surface. For the tape peeling test, 3 M tape (#600, width 25.4 mm, thickness 50  $\mu\text{m}$ ) was pressed onto the coating at a pressure of 2.5 kPa and then peeled off. The contact angle and rolling angle were measured after a specific number of cycles. In the falling water impact test, the sample was positioned 20 cm directly beneath a water tap with a flow rate of 1.12 m/s. Measurements of the contact angle and rolling angle at the impact site were taken after a designated period. During the acid and alkali salt immersion tests, as well as water immersion, the sample was submerged in solutions with pH values of 1, 7, and 12, respectively. Following immersion, measurements of the contact angle and rolling angle were conducted. UV aging was

performed by placing the coatings in an accelerated aging chamber equipped with a UVB bulb emitting light at 310 nm with an intensity of  $6 \text{ mW/cm}^2$ . Each cycle consisted of 4 h of UV irradiation at  $60^\circ\text{C}$  followed by 4 h of condensation at  $50^\circ\text{C}$ . UV irradiation was then followed by condensation at  $50^\circ\text{C}$  for an additional 4 h. After a certain number of cycles, the contact and sliding angles were measured. High- and low-temperature stability tests: First, the sample was placed in a constant-temperature oven at  $-20^\circ\text{C}$  for 10 min and then immediately put into a constant-temperature oven at  $80^\circ\text{C}$  for 10 min for one cycle after removal. After a certain cycle, the contact angle and rolling angle were measured. Delayed icing test: A  $150 \mu\text{L}$  droplet was placed in a test chamber at a temperature of  $-18^\circ\text{C}$  and a humidity of 5%. The icing time of the droplets on both the coated and uncoated samples was observed.

### 3. Results and Discussion

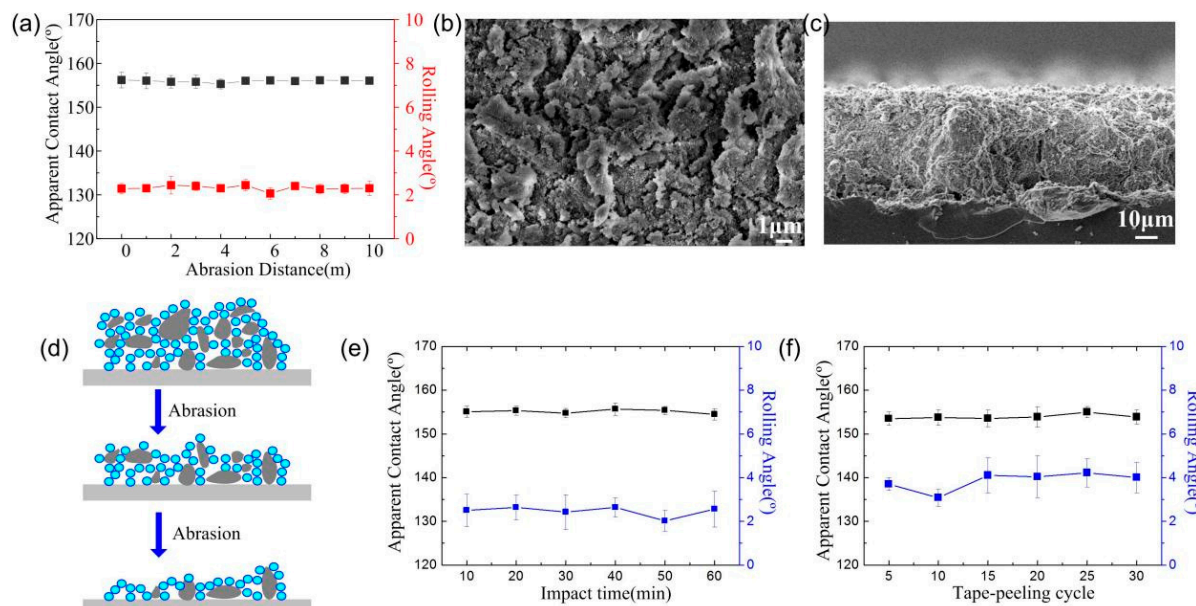
#### 3.1. Low Adhesion of Coatings

Figure 1c depicts the surface morphology of the coated sample, revealing numerous irregular micro- and nanoscale protrusions dispersed randomly across the surface. The valleys between these protrusions can entrap air, creating a liquid–air interface and resulting in the surface's superhydrophobic nature. An SEM image of the sample's cross-section in Figure 1d illustrates a top–down porous self-similar structure. This structure's advantage lies in maintaining a rough surface even if the outer layer is damaged. The coated samples demonstrate outstanding superhydrophobic properties, exhibiting a contact angle of up to  $156^\circ \pm 0.6^\circ$  and a rolling angle of  $2.3^\circ \pm 0.3^\circ$ . A water droplet adhesion experiment was conducted to evaluate the coatings' adhesion properties, as illustrated in Figure 1e. A dropper with a  $5 \mu\text{L}$  water droplet suspended at one end was lowered until the droplet adhered to the surface, and then the dropper was used to detach the droplet from the surface. The droplets were effortlessly separated from the surface, indicating low adhesion. Subsequently, the bouncing behavior of droplets on the coated surface was examined, as depicted in Figure 1f. A high-speed video camera recorded a  $5 \mu\text{L}$  droplet bouncing three times from a distance of 5 cm on the horizontally positioned coating. The droplet's bouncing height gradually decreased, ultimately reaching a stable superhydrophobic state. Thanks to the micro-nano hierarchical structure and low surface energy molecules, the prepared coatings exhibit exceptional superhydrophobicity and low adhesion properties. The adhesion force of microdroplets on the coating surface was quantitatively assessed using a high-sensitivity microelectromechanical equilibrium system, yielding an adhesion force value of  $10.8 \pm 0.4 \mu\text{N}$ .

#### 3.2. Mechanical Durability Testing of Coatings

The mechanical durability of superhydrophobic coatings significantly influences their potential practical applications. This durability was assessed through sandpaper rubbing, falling water impact, and tape peeling experiments. Abrasion resistance is a primary concern for superhydrophobic coatings. Figure 2a demonstrates the superhydrophobicity of the coating after enduring a 10 m wear distance. The contact angle remains approximately  $155^\circ$ , with a roll angle of about  $2.4^\circ$ , showing minimal change compared to pre-wear conditions and continuing to exhibit excellent wetting resistance. As shown in Figure 2b,c, many rough micro- and nanoscale structures still exist on the rubbed surface. The excellent mechanical durability of the coatings is mainly due to their low surface energy, and the newly exposed areas still have micro/nanorough structures for superhydrophobicity (Figure 2d). In comparison to other single-step spraying methods, the wear resistance is notably improved. Zhang et al. [36] utilized the single-step method for fabricating superhydrophobic coatings, which exhibited a loss of their superhydrophobic characteristics upon abrasion with 240-grit sandpaper over a distance of 0.6 m under a load of 1.6 kPa. The coating prepared by Zhi et al. [37], using the single-step method, demonstrated a gradual decrease in contact angle as friction distance increased when subjected to 300 g weights and sanded with 600-grit sandpaper. The superhydrophobic coating developed by Wei et al. [38] also

experienced a loss of its superhydrophobic properties after undergoing 20 cycles of abrasion (Taber abrasion test, 250 g load, ASTM D4060 [43]). They postulated that once the rough surface structure was damaged by the sandpaper, the inner layer transformed into a flat surface primarily composed of resin due to embedded nanoparticles within the adhesive.



**Figure 2.** (a) Effect of the sandpaper abrasion distance on the contact and roll angles; SEM images of coatings after 10 m of abrasion; (b) top view and (c) side view; (d) schematic diagram of the coating abrasion process; (e) effect of the water impingement time on the contact and roll angles; and (f) effect of the number of tape stripping cycles on the contact and roll angles.

The vulnerability of the air layer within the microstructure of superhydrophobic coatings to external water flow impact can lead to a transition from the Cassie state to the Wenzel state. The stability of this air layer can be assessed by measuring the contact angle and rolling angle of the sample surface following water flow impact. Experimental findings reveal that even after 60 min of water flow impact, the contact angle and rolling angle of the coating remained virtually unchanged, with a contact angle of approximately 155° and a rolling angle of about 3°, indicating sustained good superhydrophobicity (Figure 2e).

Tape peeling assesses the adhesion of rough structures to a substrate. The relationship between the number of tape peeling cycles and the contact angle and roll angle of the surface enables evaluation of the surface's anti-peeling properties. Results from the tape peeling test indicate that following 30 cycles, the contact angle and roll angle of the coating measured 154.2° and 4.1°, respectively (Figure 2f), demonstrating continued excellent superhydrophobicity.

### 3.3. Coating Chemical Durability Test

The stability of superhydrophobic coatings not only relies on their micro- and nano-rough structures but also necessitates the preservation of low-surface-energy properties. Therefore, maintaining the low surface energy state is crucial for the durability of these coatings. The failure of low surface energy substances can occur due to reactions with corrosive media and natural aging. The first damage mechanism, involving reactions with corrosive media, was evaluated by immersing the superhydrophobic coating samples in different pH solutions and aqueous solutions for varying durations. The results depicted in Figure 3a-d illustrate that the samples retained their superhydrophobicity even after 7 days of immersion in strong acid (pH = 1), strong alkali (pH = 12), 3.5wt% NaCl solution (pH = 7), and water. This resilience can be attributed to the chemical stability of the resins and additives, as well as the long-term effect of the air layer on the coating surface.

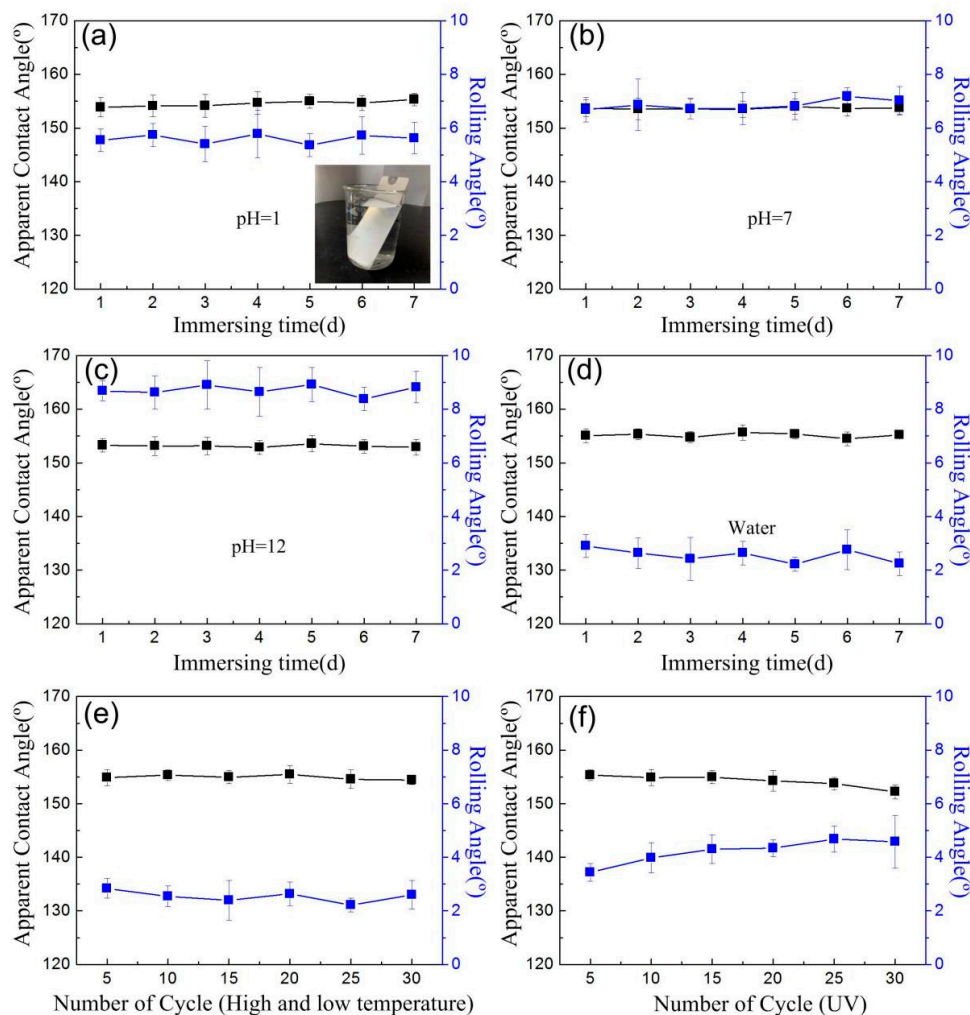


**Figure 3.** Effect of sample immersion time in (a) pH = 1, (b) pH = 7, (c) pH = 12, and (d) aqueous solutions on contact and roll angles; (e) effect of high and low-temperature testing on contact and roll angles; and (f) effect of UV irradiation on contact and roll angles.

The second damage mechanism, natural aging, was simulated by subjecting the coatings to alternating high and low temperatures and UV irradiation. Figure 3e demonstrates the minimal effect on superhydrophobicity even after 30 cycles of high and low-temperature cycling tests. Similarly, Figure 3f displays the marginal changes in contact angle and roll angle after UV aging. Following 30 aging cycles (totaling 240 h), the water contact angle and rolling angle remained approximately 152.6° and 4.8°, respectively. This resilience is attributed to the excellent chemical inertness of both the nanofillers and the organic resin.

### 3.4. Self-Cleaning and Delayed Icing Effects of the Coatings

The prepared coatings were covered with quartz sand, and the self-cleaning behavior of the water droplets (dyed blue) was recorded. As shown in Figure 4a, the quartz sand on the superhydrophobic surface was easily removed by a large number of water droplets to form a clean surface. We also conducted static anti-icing experiments. The icing process of water droplets on a sample with an initial surface temperature of  $-20^{\circ}\text{C}$  was examined. This is shown in Figure 4b. The water droplets on the surface inevitably freeze after a period of time, regardless of whether the sample is superhydrophobic. The freezing process starts at the solid–liquid interface and the water droplets gradually blur from the bottom to the top and finally condense into ice particles. The freezing time of the uncoated sample is only approximately one-third of that of the coated sample, which may be due to the

microstructure of the coated surface that traps air to retard the heat transfer between the water droplets and the frozen surface.

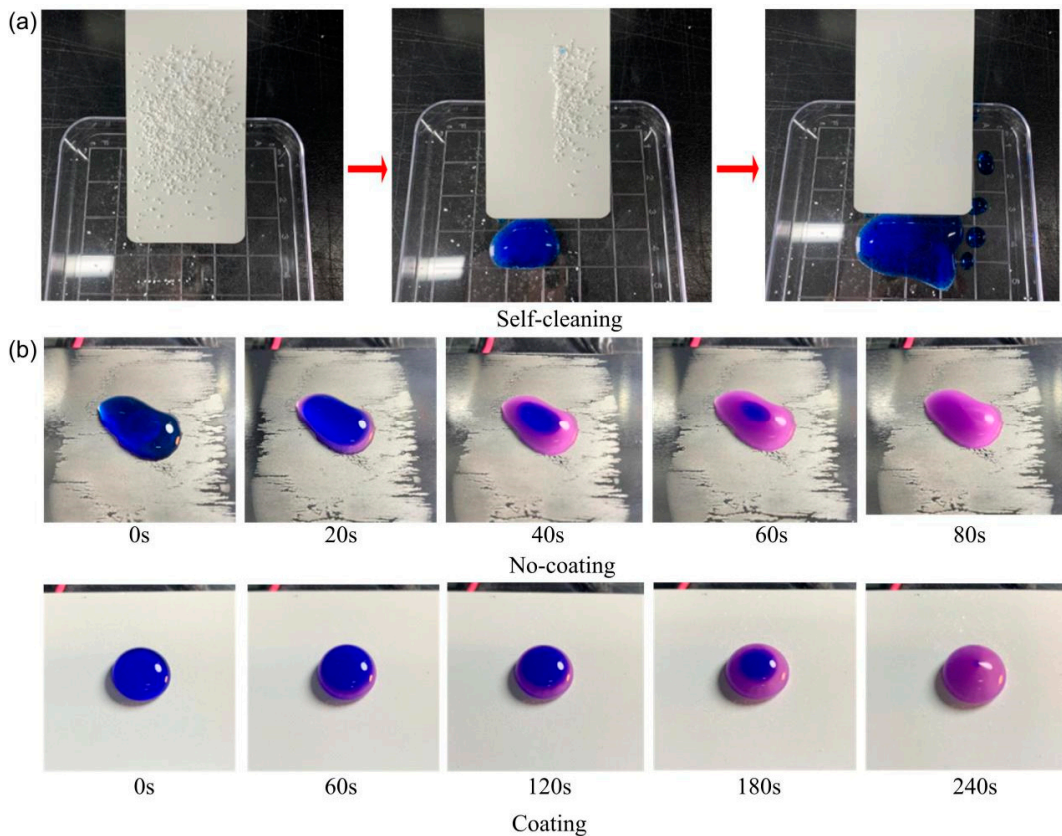


**Figure 4.** (a) Self-cleaning effect of coatings; (b) delayed icing effect of coatings.

### 3.5. The Economic Viability and Scalability

Large-scale industrial production involves two key issues. Firstly, it is important to determine whether the ratios between the raw materials in scaled-up productions are consistent with those used in the laboratory to prepare small quantities of samples. According to the experimental methodology outlined in Section 2.3, the synthesis process does not entail complex steps or chemical reactions but only simple dropwise addition and physical stirring. Therefore, it is feasible to scale up the amount of raw material precisely according to the original ratio. Secondly, it is essential to assess whether industrial equipment is available to meet production conditions. The laboratory preparation of small amounts of paint can be accomplished using a dropper and a magnetic stirrer. However, when scaling up the quantity, peristaltic pumps and mixing kettles may be necessary. It is estimated that the cost of raw materials for producing one kilogram of superhydrophobic paint is approximately RMB 200 yuan.

## 4. Conclusions

This paper presents the preparation of a superhydrophobic coating with remarkable durability using a spraying method. The coating exhibits excellent low adhesion, offering a contact angle of  $156^\circ$ , a rolling angle of  $2.2^\circ$ , and a minimal adhesion force to water droplets of only  $10.8 \pm 0.4 \mu\text{N}$ . Moreover, the coating demonstrates robust durability, maintaining its superhydrophobic properties following various tests, including sandpaper abrasion, water impact, tape peeling, immersion in acid, alkali, salt, and aqueous solutions, ultraviolet irradiation aging, as well as high and low-temperature aging. The combination of micro-spheres formed through undesirable solvent phase separation of the resin and fluorinated  $\text{SiO}_2$  nanoparticles results in a top-down self-similar porous structure, contributing to the

coating's durability. This method is straightforward and suitable for large-scale preparation, offering a novel approach for the practical applications of superhydrophobic coatings in areas such as anti/de-icing, self-cleaning, anti-corrosion, and drag reduction. Moving forward, we will persist in optimizing both the preparation methods and the materials employed to achieve superhydrophobic coatings with enhanced durability.

**Author Contributions:** Writing—original draft, X.L.; supervision, X.L. and L.W.; project administration, X.L.; funding acquisition, X.L.; validation, Z.Z. and Z.L.; investigation, S.J.; formal analysis, M.C.; writing—review and editing, Z.Z., Z.L., S.J., M.C. and L.W. All authors have read and agreed to the published version of the manuscript.

**Funding:** The authors acknowledge the support from the National Science Foundation of China (Grant No. 22203038); Aeronautical Science Foundation of China (No. 20230054072017); Doctoral Research start-up fund: XQB202027; Youth Foundation of Hebei Education Committee: QN2019147, QN2024097; and School-level Research Project of Langfang Normal University: XKF202001.

**Institutional Review Board Statement:** Not applicable.

**Informed Consent Statement:** Not applicable.

**Data Availability Statement:** All data that support the findings of this study are included within this article.

**Conflicts of Interest:** The authors declare no conflicts of interest.

## References

- Peng, C.; Chen, Z.; Tiwari, M.K. All-organic superhydrophobic coatings with mechanochemical robustness and liquid impalement resistance. *Nat. Mater.* **2018**, *17*, 355–360. [[CrossRef](#)]
- Feng, K.; Hung, G.; Liu, J.; Li, M.; Zhou, C.; Liu, M. Fabrication of high performance superhydrophobic coatings by spray-coating of polysiloxane modified halloysite nanotubes. *Chem. Eng. J.* **2018**, *331*, 744–754. [[CrossRef](#)]
- Zhang, S.; Huang, J.; Chen, Z.; Lai, Y. Bioinspired Special Wettability Surfaces: From Fundamental Research to Water Harvesting Applications. *Small* **2017**, *13*, 1602992. [[CrossRef](#)]
- Li, M.; Liu, W.; Yin, Z.; Yang, H.; Chen, Y.; Yang, C.; Luo, Y.; Hong, Z.; Xie, C.; Xue, M. Facile fabrication of superhydrophobic and photocatalytic self-cleaning flexible strain sensor membrane for human motion. *Sens. Actuators A Phys.* **2023**, *363*, 114750. [[CrossRef](#)]
- Qing, Y.; Shi, S.; Lv, C.; Zheng, Q. Microskeleton-nanofiller composite with mechanical super-robust superhydrophobicity against abrasion and impact. *Adv. Funct. Mater.* **2020**, *30*, 1910665. [[CrossRef](#)]
- Zhang, M.; Wang, P.; Sun, H.; Wang, Z. Superhydrophobic surface with hierarchical architecture and bimetallic composition for enhanced antibacterial activity. *ACS Appl. Mater. Interfaces* **2014**, *6*, 22108–22115. [[CrossRef](#)]
- Zhang, X.; Wang, L.; Levänen, E. Superhydrophobic surfaces for the reduction of bacterial adhesion. *RSC Adv.* **2013**, *3*, 12003–12020. [[CrossRef](#)]
- Wang, H.; He, M.; Liu, H.; Guan, Y. One-Step Fabrication of Robust Superhydrophobic Steel Surfaces with Mechanical Durability, Thermal Stability, and Anti-icing Function. *ACS Appl. Mater. Interfaces* **2019**, *11*, 25586–25594. [[CrossRef](#)]
- Li, X.; Wang, G.; Moita, A.; Zhang, C.; Wang, S.; Liu, Y. Fabrication of bio-inspired non-fluorinated superhydrophobic surfaces with anti-icing property and its wettability transformation analysis. *Appl. Surf. Sci.* **2020**, *505*, 144386. [[CrossRef](#)]
- Park, H.; Choi, C.; Kim, C. Superhydrophobic drag reduction in turbulent flows: A critical review. *Exp. Fluids* **2021**, *62*, 229. [[CrossRef](#)]
- Liravi, M.; Pakzad, H.; Moosavi, A.; Nouri-Borujerdi, A. A comprehensive review on recent advances in superhydrophobic surfaces and their applications for drag reduction. *Prog. Org. Coat.* **2020**, *140*, 105537. [[CrossRef](#)]
- Dhyani, A.; Wang, J.; Halvey, A.; Macdonald, B.; Mehta, G.; Tuteja, A. Design and applications of surfaces that control the accretion of matter. *Science* **2021**, *373*, eaba5010. [[CrossRef](#)]
- Yin, Z.; Li, Z.; Deng, Y.; Xue, M.; Chen, Y.; Ou, J.; Xie, Y.; Luo, Y.; Xie, C.; Hong, Z. Multifunctional CeO<sub>2</sub>-coated pulp/cellulose nanofibers (CNFs) membrane for wastewater treatment: Effective oil/water separation, organic contaminants photodegradation, and anti-bioadhesion activity. *Ind. Crops Prod.* **2023**, *197*, 116672. [[CrossRef](#)]
- Yin, Z.; Li, M.; Li, Z.; Deng, Y.; Xue, M.; Chen, Y.; Ou, J.; Lei, S.; Luo, Y.; Xie, C. A harsh environment resistant robust Co(OH)<sub>2</sub>@stearic acid nanocellulose-based membrane for oil-water separation and wastewater purification. *J. Environ. Manag.* **2023**, *342*, 118127. [[CrossRef](#)]
- Chen, X.; Yin, Z.; Deng, Y.; Li, Z.; Xue, M.; Chen, Y.; Xie, Y.; Liu, W.; He, P.; Luo, Y.; et al. Harsh environment-tolerant and robust superhydrophobic graphenebased composite membrane for wearable strain sensor. *Sens. Actuators A Phys.* **2023**, *362*, 114630. [[CrossRef](#)]

16. Lin, Y.; Han, J.; Cai, M.; Liu, W.; Luo, X.; Zhang, H.; Zhong, M. Durable and robust transparent superhydrophobic glass surfaces fabricated by a femtosecond laser with exceptional water repellency and thermostability. *J. Mater. Chem. A* **2018**, *6*, 9049–9056. [[CrossRef](#)]
17. Pan, L.; Dong, H.; Bi, P. Facile preparation of superhydrophobic copper surface by  $\text{HNO}_3$  etching technique with the assistance of CTAB and ultrasonication. *Appl. Surf. Sci.* **2010**, *257*, 1707–1711. [[CrossRef](#)]
18. Long, M.; Peng, S.; Chen, J.; Yang, X.; Deng, W. A new replication method for fabricating hierarchical polymer surfaces with robust superhydrophobicity and highly improved oleophobicity. *Colloids Surf. A* **2016**, *507*, 7–17. [[CrossRef](#)]
19. Chen, Y.; Zhang, Y.; Shi, L.; Li, J.; Xin, Y.; Yang, T.; Guo, Z. Transparent superhydrophobic/superhydrophilic coatings for self-cleaning and anti-fogging. *Appl. Phys. Lett.* **2012**, *101*, 033701. [[CrossRef](#)]
20. Burkarter, E.; Saul, C.K.; Thomazi, F.; Cruz, N.C.; Roman, L.S.; Schreiner, W.H. Superhydrophobic electrosprayed PTFE. *Surf. Coat. Technol.* **2007**, *202*, 194–198. [[CrossRef](#)]
21. Duan, Z.; Qu, L.; Hu, Z.; Liu, D.; Liu, R.; Zhang, Y.; Zheng, X.; Zhang, J.; Wang, X.; Zhao, G. Fabrication of micro-patterned  $\text{ZrO}_2/\text{TiO}_2$  composite surfaces with tunable super-wettability via a photosensitive sol-gel technique. *Appl. Surf. Sci.* **2020**, *529*, 147136. [[CrossRef](#)]
22. Singh, A.; Singh, J. Fabrication of durable superhydrophobic coatings on cotton fabrics with photocatalytic activity by fluorine-free chemical modification for dual-functional water purification. *New J. Chem.* **2017**, *41*, 4618–4628. [[CrossRef](#)]
23. Zhang, X.; Zheng, F.; Ye, L.; Xiong, P.; Yan, L.; Yang, W.; Jiang, B. A one-pot sol-gel process to prepare a superhydrophobic and environment-resistant thin film from ORMOSIL nanoparticles. *RSC Adv.* **2014**, *4*, 9838–9841. [[CrossRef](#)]
24. Darband, G.; Aliofkazraei, M.; Khorsand, S.; Sokhanvar, S.; Kaboli, A. Science and engineering of superhydrophobic surfaces: Review of corrosion resistance, chemical and mechanical stability. *Arab. J. Chem.* **2020**, *13*, 1763–1802. [[CrossRef](#)]
25. Zhao, Y.; Tang, Y.; Wang, X.; Lin, T. Superhydrophobic cotton fabric fabricated by electrostatic assembly of silica nanoparticles and its remarkable buoyancy. *Appl. Surf. Sci.* **2010**, *256*, 6736–6742. [[CrossRef](#)]
26. Wang, S.; Xue, Y.; Ban, C.; Xue, Y.; Taleb, A.; Jin, Y. Fabrication of robust tungsten carbide particles reinforced Co-Ni superhydrophobic composite coating by electrochemical deposition. *Surf. Coat. Technol.* **2020**, *385*, 125390. [[CrossRef](#)]
27. Zhang, B.; Zhao, X.; Li, Y.; Hou, B. Fabrication of durable anticorrosion superhydrophobic surfaces on aluminum substrates via a facile one-step electrodeposition approach. *RSC Adv.* **2016**, *6*, 35455–35465. [[CrossRef](#)]
28. Ghasemlou, M.; Daver, F.; Ivanova, E.; Adhikari, B. Bio-inspired sustainable and durable superhydrophobic materials: From nature to market. *J. Mater. Chem. A* **2019**, *7*, 16643–16670. [[CrossRef](#)]
29. Wu, L.; Zhang, J.; Li, B.; Fan, L.; Li, L.; Wang, A. Facile preparation of super durable superhydrophobic materials. *J. Colloid Interface Sci.* **2014**, *432*, 31–42. [[CrossRef](#)]
30. Motamedi, M.; Warkiani, M.; Taylor, R. Transparent surfaces inspired by nature. *Adv. Opt. Mater.* **2018**, *6*, 1800091. [[CrossRef](#)]
31. Wang, D.; Sun, Q.; Hokkanen, M.; Zhang, C.; Lin, F.; Liu, Q.; Zhu, S.; Zhou, T.; Chang, Q.; He, B.; et al. Design of robust superhydrophobic surfaces. *Nature* **2020**, *582*, 55–59. [[CrossRef](#)]
32. Chen, B.; Qiu, J.; Sakai, E.; Kanazawa, N.; Liang, R.; Feng, H. Robust and superhydrophobic surface modification by a “Paint + Adhesive” method: Applications in self-cleaning after oil contamination and oil–water separation. *ACS Appl. Mater. Interfaces* **2016**, *8*, 17659–17667. [[CrossRef](#)] [[PubMed](#)]
33. Xue, F.; Shi, X.; Bai, W.; Li, J.; Li, Y.; Zhu, S.; Liu, Y.; Feng, L. Enhanced durability and versatile superhydrophobic coatings via facile one-step spraying technique. *Colloids Surf. A* **2022**, *640*, 128411. [[CrossRef](#)]
34. Zhang, F.; Qian, H.; Wang, L.; Wang, Z.; Du, C.; Li, X.; Zhang, D. Superhydrophobic carbon nanotubes/epoxy nanocomposite coating by facile one-step spraying. *Surf. Coat. Technol.* **2018**, *341*, 15–23. [[CrossRef](#)]
35. Huang, J.; Cai, P.; Li, M.; Wu, Q.; Li, Q.; Wang, S. Preparation of CNF/PDMS Superhydrophobic Coatings with Good Abrasion Resistance Using a One-Step Spray Method. *Materials* **2020**, *13*, 5380. [[CrossRef](#)]
36. Zhang, L.; Xue, X.; Zhang, H.; Huang, Z.; Zhang, Z. Superhydrophobic surface with excellent mechanical robustness, water impact resistance and hydrostatic pressure resistance by two-step spray-coating technique. *Compos. Part A Appl. Sci. Manuf.* **2021**, *146*, 106405. [[CrossRef](#)]
37. Zhi, D.; Lu, Y.; Sathasivam, S.; Parkin, I.; Zhang, X. Large-scale fabrication of translucent and repairable superhydrophobic spray coatings with remarkable mechanical, chemical durability and UV resistance. *J. Mater. Chem. A* **2017**, *5*, 10622–10631. [[CrossRef](#)]
38. Wei, J.; Li, B.; Tian, N.; Zhang, J.; Liang, W.; Zhang, J. Scalable Robust Superamphiphobic Coatings Enabled by Self-Similar Structure, Protective Micro-Skeleton, and Adhesive for Practical Anti-Icing of High-Voltage Transmission Tower. *Adv. Funct. Mater.* **2022**, *32*, 2206014. [[CrossRef](#)]
39. Carreño, F.; Gude, M.R.; Calvo, S.; De La Fuente, O.R.; Carmona, N. Synthesis and characterization of superhydrophobic surfaces prepared from silica and alumina nanoparticles on a polyurethane polymer matrix. *Prog. Org. Coat.* **2019**, *135*, 205–212. [[CrossRef](#)]
40. Zhang, H.; Bu, X.; Li, W.; Cui, M.; Ji, X.; Tao, F.; Gai, L.; Jiang, H.; Liu, L.; Wang, Z. A Skin-Inspired Design Integrating Mechano-Chemical-Thermal Robustness into Superhydrophobic Coatings. *Adv. Mater.* **2022**, *34*, 2270229. [[CrossRef](#)]
41. Lu, Y.; Sathasivam, S.; Song, J.; Crick, C.; Carmalt, C.; Parkin, I. Repellent materials. Robust self-cleaning surfaces that function when exposed to either air or oil. *Science* **2021**, *590*, 301–310.

42. Xin, L.; Li, H.; Gao, J.; Wang, Z.; Zhou, K.; Yu, S. Large-scale fabrication of decoupling coatings with promising robustness and superhydrophobicity for antifouling, drag reduction, and organic photodegradation. *Friction* **2023**, *11*, 716–736. [[CrossRef](#)]
43. ASTM D4060-19; Standard Test Method for Abrasion Resistance of Organic Coatings by the Taber Abraser. ASTM International: West Conshohocken, PA, USA, 2019.

**Disclaimer/Publisher's Note:** The statements, opinions and data contained in all publications are solely those of the individual author(s) and contributor(s) and not of MDPI and/or the editor(s). MDPI and/or the editor(s) disclaim responsibility for any injury to people or property resulting from any ideas, methods, instructions or products referred to in the content.